

Detection of charged Higgs bosons through the rare decay $H^+ \rightarrow W^+ \gamma$

Sreerup Raychaudhuri¹

International Centre for Theoretical Physics, I-34100 Trieste, Italy

and

Amitava Raychaudhuri

Department of Pure Physics, University of Calcutta, 92 Acharya Prafulla Chandra Road, Calcutta 700 009, India

Received 31 July 1992

The process $H^+ \rightarrow W^+ \gamma$ is evaluated exactly in the 't Hooft–Feynman gauge in a two-Higgs doublet model with scalar masses and couplings as in the minimal supersymmetric standard model. At hadron colliders this rare decay might provide a clean signal for detection of charged Higgs particles lighter than the top quark.

Since LEP and SLC have commenced running, the standard electroweak model stands unsurpassed as the best theory of fundamental interactions to date. This imposing structure, however, stands on an uncertain foundation – the scalar sector. Not only has the scalar Higgs boson of the standard model (SM) eluded experimental detection but the very structure of this sector seems ad hoc. There are four gauge bosons in the theory, six quarks (in three colours each) and six leptons, while, remarkably, there is only one elementary scalar. Almost any extension of the SM – barring technicolour – requires additional scalar multiplets. After the Higgs mechanism, there are generally one or more pairs of physical *charged* Higgs bosons and neutral scalars. Probably the best example of a model in which there are charged Higgs bosons is the minimal supersymmetric standard model (MSSM). In this model the physical scalar spectrum consists of [1] a pair of charged Higgs bosons H^\pm , and three neutrals – a pair of *CP*-even bosons H^0, h^0 and a *CP*-odd scalar A^0 . The masses and couplings of these particles can be expressed in terms of just two free parameters, which we choose to be the mass of the charged Higgs boson m_+ and the ratio of the vacuum expectation values $\tan \beta = v_2/v_1$. In the MSSM, the H^+ is heavier than the W , satisfying

$$m_+^2 = m_W^2 + m_A^2. \quad (1)$$

Consequently, production of charged Higgs particles at LEP II through the process $e^+e^- \rightarrow \gamma^* \rightarrow H^+H^-$ or $Z^{0*} \rightarrow H^+H^-$ will be kinematically suppressed or disallowed. For direct production of these particles in the near future, then, one must turn to hadron colliders. One must distinguish between two possibilities:

(i) $m_t + m_b < m_+$: The charged Higgs are produced [2] by $g\bar{b} \rightarrow \bar{t}H^+$ or $\bar{b}t \rightarrow H^+$. These processes are rendered viable because the $t\bar{b}H^-$ vertex is enhanced by the factor m_t/m_W . It has been estimated [2] that they could result in the production of 10^6 charged Higgs particles per year at the SSC with a luminosity of $10^4 \text{ pb}^{-1}/\text{yr}$. At the LHC, the number could be of the same order of magnitude because the higher luminosity may compensate for the lower \sqrt{s} [3]. The dominant decay mode will be $H^+ \rightarrow t\bar{b}$ where the same factor m_t/m_W is responsible for enhancing the corresponding branching ratio. This hadronic signal will be *completely obliterated* by the QCD

¹ Permanent address: Department of Pure Physics, University of Calcutta, 92 Acharya Prafulla Chandra Road, Calcutta 700 009, India.

background. The mode we examine, $H^+ \rightarrow W^+ \gamma$, though possessing a small branching ratio in this case, might provide a cleaner alternative.

(ii) $m_t + m_b > m_+$: In this case, on which we focus, the dominant production channel is through top quark decay. The branching ratio to H^+ is a function of $\tan \beta$ and for $\tan \beta = 2$ can lead to 1.4×10^7 (7×10^7) charged Higgs per year at the SSC (LHC) assuming a luminosity of 10^4 pb^{-1}/yr (5×10^5 pb^{-1}/yr). We use these as our benchmark figures. The principal decay modes, in this case, $H^+ \rightarrow W^+ h^0$, $H^+ \rightarrow c\bar{s}$, $H^+ \rightarrow \tau^+ \nu_\tau$ are plagued by large backgrounds. Perhaps a good bet would be to look for violations of universality in the lepton spectrum, but this can result [4] in large uncertainties since universality violation can arise from other sources as well (such as mixing with a heavy vector doublet of fermions). In view of such problems, it is useful to turn to rare decay modes.

The rare decay $H^+ \rightarrow W^+ \gamma$ has been suggested as one such process since it will result in a mono-energetic photon of frequency

$$\omega = \frac{m_+^2 - m_W^2}{2m_+}. \quad (2)$$

The principal background to this, which comes from $q\bar{q} \rightarrow W^+ \gamma$, can be brought under control [5] by imposing cuts on the rapidity of the emerging photon.

Unfortunately, the coupling $W^+ H^- \gamma$ cannot exist at the tree-level because of electromagnetic gauge invariance [6]. Its form must be $iM_{\mu\nu} \epsilon_W^\mu(p_1) \epsilon^\nu(p_2)$ where $M_{\mu\nu} = \lambda g m_W g_{\mu\nu}$ at the tree-level, since it arises from the covariant derivative. Electromagnetic gauge invariance demands that $p_2^\nu M_{\mu\nu} = 0$ implying $\lambda = 0$. At the one-loop level, however, $M_{\mu\nu}$ can have the general Lorentz structure

$$M_{\mu\nu} = F_1 g_{\mu\nu} + F_2 p_{1\nu} p_{2\mu} + F_3 \epsilon_{\mu\nu\alpha\beta} p_1^\alpha p_2^\beta \quad (3)$$

taking into account transversality of the polarisation vectors. Electromagnetic gauge invariance now merely demands that the form factors $F_{1,2}$ satisfy the identity

$$F_1 + F_2 p_1 \cdot p_2 = 0. \quad (4)$$

In this letter we report the first complete calculation of the $W^+ H^- \gamma$ coupling at one loop in the 't Hooft-Feynman gauge for the MSSM^{#1}. Previous estimates of this amplitude have either been in the cumbersome unitary gauge [5] or have retained only quark loop contributions and/or used approximations to obtain simple analytic results [7]. We have developed a calculation technique in which the contribution of each Feynman diagram can be written as a linear combination of scalar one-, two- and three-point functions [8,9]. The canonical requirements of finiteness and gauge invariance of the net amplitude then provide excellent cross-checks of these expressions since the one-, two- and three-point functions with different arguments are linearly independent and hence cancel out separately when the form factors in eq. (4) are expressed in terms of these.

Before we enumerate the Feynman diagrams and the amplitudes corresponding to this process, it is necessary to explain some notations and conventions which have been used to express these results. Scalar one-, two- and three-point functions are defined, respectively, by (all integrations being in euclidean space)

$$A(m) \equiv \frac{1}{\pi^2} \int d^4q \frac{1}{q^2 + m^2}, \quad B_e(m_1, m_2; M) \equiv \frac{1}{\pi^2} \int d^4q \frac{1}{(q^2 + m_1^2)[(q+p)^2 + m_2^2]}, \quad (5)$$

where $p^2 = M^2$.

$$C_0(m_1, m_2, m_3; M_1, M_2, M_3) \equiv \frac{1}{\pi^2} \int d^4q \frac{1}{(q^2 + m_1^2)[(q+p_1)^2 + m_2^2][(q+p_1+p_2)^2 + m_3^2]}, \quad (6)$$

^{#1} It has been shown [7] that sparticle contributions to the $H^+ \rightarrow W^+ \gamma$ amplitude are not significantly large. Hence this result can be taken as a pretty good approximation to the complete MSSM amplitude.

where $(p_1 + p_2)^2 = M_1^2$, $p_1^2 = M_2^2$, $p_2^2 = M_3^2$.

Vector two- and three-point functions are defined by

$$B_\mu(m_1, m_2; M) \equiv \frac{1}{\pi^2} \int d^4q \frac{q_\mu}{(q^2 + m_1^2)[(q+p)^2 + m_2^2]} \equiv p_\mu B_1(m_1, m_2; M) \quad (7)$$

and $[C \equiv C_\mu(m_1, m_2, m_3; M_1, M_2, M_3)]$

$$C_\mu \equiv \frac{1}{\pi^2} \int d^4q \frac{q_\mu}{(q^2 + m_1^2)[(q+p_1)^2 + m_2^2][(q+p_1+p_2)^2 + m_3^2]} \equiv p_{1\mu} C_{11} + p_{2\mu} C_{12}. \quad (8)$$

Tensor three-point functions are defined by

$$C_{\mu\nu} \equiv \frac{1}{\pi^2} \int d^4q \frac{q_\mu q_\nu}{(q^2 + m_1^2)[(q+p_1)^2 + m_2^2][(q+p_1+p_2)^2 + m_3^2]} \\ \equiv p_{1\mu} p_{1\nu} C_{21} + p_{2\mu} p_{2\nu} C_{22} + (p_{1\mu} p_{2\nu} + p_{2\mu} p_{1\nu}) C_{23} + \delta_{\mu\nu} C_{24}. \quad (9)$$

The form factors B_1 , C_{11} , C_{12} , C_{21} , C_{22} , C_{23} and C_{24} can all be written [9] as linear combinations of the basic functions A , B_0 and C_0 . Furthermore, in order to prove gauge invariance of the amplitudes given in the text, we require the following two identities:

$$2B_1(m_1, m_2; M) + B_0(m_1, m_2; M) = \frac{1}{M^2} [A(m_2) - A(m_1)] - \frac{m_1^2 - m_2^2}{M^2} B_0(m_1, m_2; M). \quad (10)$$

For $C_A = C_A(m_1, m_1, m_3, M_1, 0, M_3)$, with $A = 22, 23, 24$,

$$4C_{24} + 4p_1 \cdot p_2 (C_{23} - C_{22}) = \frac{1}{M_3^2} [A(m_3) - A(m_1) + (M_3^2 + m_3^2 - m_1^2) B_0(m_1, m_3; M_3)]. \quad (11)$$

These can be derived from the formulae given in ref. [9] which express all form factors in terms of A , B_0 and C_0 .

The Feynman diagrams contributing to the $W^+ H^- \gamma$ amplitude at the one-loop level in the 't Hooft-Feynman gauge are given in fig. 1. The couplings of charged Higgs bosons to positively charged fermions f being proportional to m_f/m_W , we have not shown the contributions of loops with either quarks belonging to the first two generations or with leptons in the internal lines. (We have, however, included them in our numerical calculations and verified that their contributions are always less than one percent of the total.) Amplitudes with top and bottom quarks in the loops form a gauge-invariant set and are illustrated in fig. 1a. There are ten diagrams which add up to give

$$M_{\mu\nu} = \frac{-\alpha^{3/2} m_W}{2\sqrt{\pi} \sin^2 \theta_w} [F_{1f} g_{\mu\nu} + F_{2f} p_{1\nu} p_{2\mu} + F_{3f} \epsilon_{\mu\nu\alpha\beta} p^{\alpha 1} p^{\beta 2}], \quad (12)$$

where the form factors $F_{1f, 2f, 3f}$ can be expressed in terms of the one-, two- and three-point functions defined above as

$$F_{1f} = m_W^2 (x_+ - 1) [x_t C_0(t, t, b) - \frac{1}{2} x_b C_0(b, b, t)] + \frac{1}{2} S [8C_{24}(t, t, b) - 4C_{24}(b, b, t) - B_0(b, t; +)] \\ + \frac{3}{2} D B_0(b, t; W) - [\frac{3}{2} (x_+ - 1)]^{-1} \\ \times \left[\left(2x_b + D x_+ - \frac{S(D - S \cos 2\beta)}{\sin 2\beta} \right) B_0(b, t; +) + 2S B_1(b, t; +) - \frac{S[A(t) - A(b)]}{m_W^3} \right], \quad (13)$$

$$F_{2f} = -4S \{ [C_{23}(t, t, b) - C_{22}(t, t, b)] - \frac{1}{2} [C_{23}(b, b, t) - C_{22}(b, b, t)] \} \\ + 2D [C_{12}(t, t, b) - \frac{1}{2} C_{12}(b, b, t)] + [2x_t C_0(t, t, b) - x_b C_0(b, b, t)], \quad (14)$$

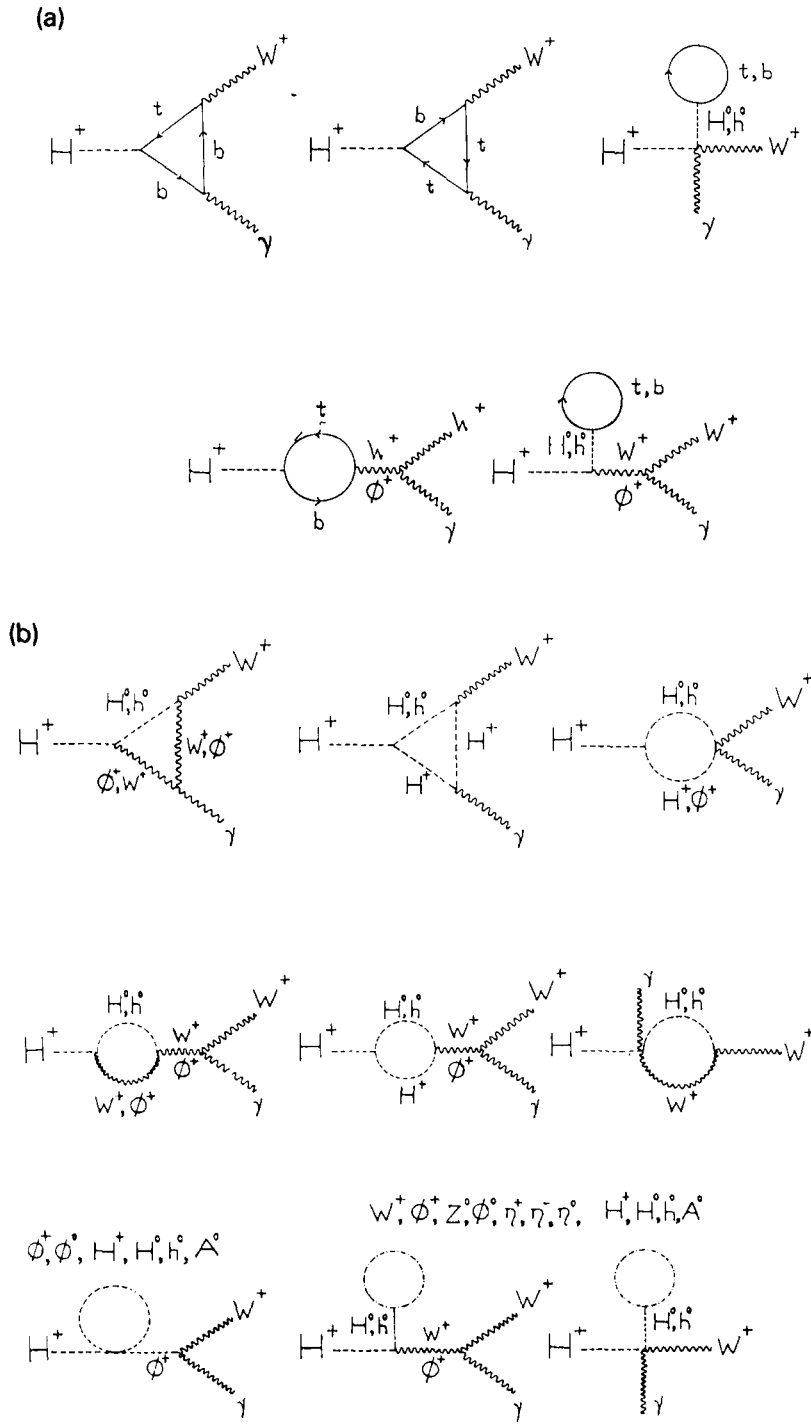


Fig. 1. Complete set of diagrams (a) from fermions and (b) from bosons contributing to the process $H^+ \rightarrow W^+ \gamma$ in the 't Hooft-Feynman gauge.

$$F_{3f} = 2x_t C_0(t, t, b) + x_b C_0(b, b, t) + 2x_b C_{11}(b, b, t) + 2SC_{12}(t, t, b) + DC_{12}(b, b, t), \quad (15)$$

with $x_i = m_i^2/m_W^2$ excepting $x_t = m_t^2 \cot \beta/m_W^2$, $x_b = m_b^2 \tan \beta/m_W^2$ and $S, D = x_t \pm x_b$. All C -functions above have external masses $M_1 = m_W, M_2 = 0, M_3 = m_+$ which are not exhibited. The arguments i, j, k shown correspond to the internal masses m_i, m_j, m_k .

Contributions from gauge-bosons W^\pm, Z^0 , Higgs scalars H^\pm, H^0, h^0, A^0 , Goldstone bosons ϕ^\pm, ϕ^0 and Fadeev-Popov ghosts η^\pm, η^Z form another gauge-invariant set and are illustrated in fig. 1b. There are 100 diagrams which add up to give

$$M_{\mu\nu} = \frac{-\alpha^{3/2} m_W}{4\sqrt{\pi} \sin^2 \theta_w} \sin 2(\alpha - \beta) (F_{1b} g_{\mu\nu} + F_{2b} p_{1\nu} p_{2\mu} + F_{3b} \epsilon_{\mu\nu\alpha\beta} p_1^\alpha p_2^\beta), \quad (16)$$

where the form factors $F_{1b,2b,3b}$ can be expressed in terms of the one-, two- and three-point functions defined above as

$$\begin{aligned} F_{1b} = & \left[m_W^3 (x_+ - 1) C_0(W, W, H) + (1 + x_+ - x_H) \cdot \frac{1}{2} \left(2C_{24}(W, W, H) + \frac{B_1(W, H; +)}{x_+ - 1} \right) \right. \\ & + (x_H - 2) \cdot \frac{1}{4} \left(\frac{2B_1(+, H; +) + (x_H - 2)[B_0(W, H; +) - B_0(+, H; +)]}{x_+ - 1} + 4C_{24}(+, +, H) \right) \\ & \left. - \frac{1}{4} (x_+ + 3) B_0(W, H; +) + B_0(W, H; W) - \frac{A(m_H) - x_H[A(m_+) - A(m_W)]/(x_+ - 1)}{4m_W^2} \right] - (m_H \leftrightarrow m_h), \end{aligned} \quad (17)$$

$$\begin{aligned} F_{2b} = & \{ 2C_0(W, W, H) - (x_+ - x_H + 1) [C_{22}(W, W, H) - C_{22}(W, W, H)] \\ & - (x_H - 2) [C_{23}(+, +, H) - C_{22}(+, +, H)] \} - (m_H \leftrightarrow m_h), \end{aligned} \quad (18)$$

$$F_{3b} = 0. \quad (19)$$

These two contributions are separately finite and gauge invariant. Finiteness is checked quite trivially. In the dimensional regularisation scheme, the only A, B, C functions with divergent parts are A, B_0, B_1 , and C_{24} with

$$-\text{div } A(m)/m^2 = \text{div } B_0 = -2 \text{div } B_1 = 4 \text{div } C_{24} = A, \quad (20)$$

where $A = 2/(4-d) + \gamma - \log \pi$ (γ is the Euler-Mascheroni constant). Using the above it is simple to check that $\text{div } F_{1f} = \text{div } F_{1b} = 0$ while the other form factors are finite anyway.

Proving gauge invariance is more subtle. One has to substitute eqs. (6) and (7) or (10) and (11) in the LHS of eq. (4) and use the identities (10) and (11). This yields a linear combination of one-, two- and three-point functions with different arguments which cancel out separately. We have checked both analytically and numerically for every set of the input parameters the identities

$$F_{1f} + F_{2f} p_1 \cdot p_2 = 0, \quad \text{and} \quad F_{1b} + F_{2b} p_1 \cdot p_2 = 0. \quad (21)$$

The decay width for $H^+ \rightarrow W^+ \gamma$ is

$$\Gamma(H^+ \rightarrow W^+ \gamma) = \frac{\alpha^3 m_W (x_+ - 1)}{256 \pi^2 \sin^2 \theta_w x_+^{3/2}} |\vec{M}|^2, \quad (22)$$

where

$$|\vec{M}|^2 = 20 |F_1|^2 + 8 m_W^2 (x_+ - 1) \text{Re}(F_1^* F_2) + m_W^4 (x_+ - 1)^2 (|F_2|^2 + 2|F_3|^2), \quad (23)$$

where $F_i = F_{if} + \frac{1}{2} \sin 2(\alpha - \beta) F_{ib}$ for $i = 1, 2, 3$. The branching ratio can then be calculated using the three-level

decay widths for $H^+ \rightarrow t\bar{b}$, $W^+ h^0$, $c\bar{s}$, $\tau^+ \nu_\tau$.

For our calculations, we have used m_+ and $\tan \beta$ as free parameters. The masses of the neutral scalars and the mixing angle α are obtained using #2 eq. (1) and

$$m_{H,h}^2 = \frac{1}{2} [m_Z^2 + m_A^2 \pm \sqrt{(m_Z^2 + m_A^2)^2 - 4m_A^2 \cos^2 2\beta}], \quad \tan 2\alpha = \frac{m_A^2 + m_Z^2}{m_A^2 - m_Z^2} \tan 2\beta. \quad (24)$$

We have taken the mass of the bottom quark to be 5 GeV and other quark masses consistent with ref. [11]. It turns out, unexpectedly, that *bosonic loops contribute a negligible amount* to the final amplitude, the top quark contribution being one or two orders of magnitude larger. Although individual bosonic diagrams have contributions as large as or even larger than the top quark diagrams, there are large cancellations [12] between the different diagrams and the final result is small. In fact, with purely bosonic contributions, the branching ratio is always of the order of 10^{-8} , which obviously reinforces the conclusion of ref. [5] that the branching ratio $\leq 5 \times 10^{-5}$ with $m_t = 40$ GeV. However, with $91 \leq m_t \leq 200$ GeV this amplitude is pushed up by three to four orders of magnitude. Our calculations, in which all masses are kept at the known values, lead to a branching ratio for $m_+ < m_t$ nearly an order of magnitude greater than that estimated in ref. [7] where results are presented with only quark loops and for $m_+ > m_t$. Our results agree in the common regime.

The branching ratio of $H^+ \rightarrow W^+ \gamma$ is shown in figs. 2 and 3 for top quark masses 150 GeV and 200 GeV respectively and $\tan \beta = 2.5$. We have checked that for $2 \leq \tan \beta \leq 10$, the variation in the branching ratio is rather small and remains confined within the same order of magnitude. Full details will be given elsewhere [12]. In order to identify this mode, in addition to the detection of the photon the W emanating from the decay needs to be tagged through semileptonic decays to e or μ , reducing the signal to about one-fifth. Thus, in order to see five distinct events in a year's run at the LHC (SSC), the branching ratio must be $\geq 4 \times 10^{-7}$ (2×10^{-6}) for our benchmark figures for the H^+ production rate given earlier. A glance at figs. 2 and 3 will show that for a charged Higgs boson of mass 80–90 GeV, this is not achieved for the SSC mainly because of the limited phase space available. The branching ratio then grows steadily upto $m_+ = 135$ GeV, where it is as large as 7×10^{-4} . At this

#2 It should be noted that these are tree-level results [10]. It is now known that for a heavy top, m_t after loop corrections could be greater than m_Z .

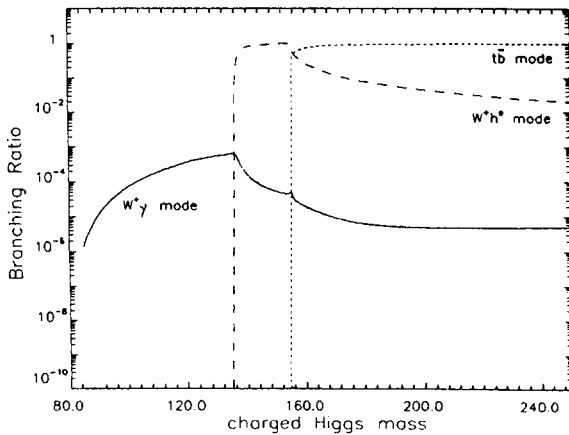


Fig. 2. Branching ratios for the decay of a charged Higgs for $m_t = 150$ GeV and $\tan \beta = 2.5$. Solid, dashed and dotted lines correspond to the decay modes $H^+ \rightarrow W^+ \gamma$, $H^+ \rightarrow W^+ h^0$, $H^+ \rightarrow t\bar{b}$.

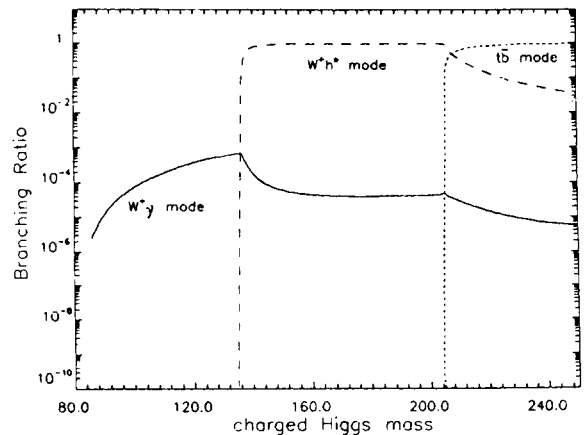


Fig. 3. Branching ratios for the decay of a charged Higgs for $m_t = 200$ GeV and $\tan \beta = 2.5$. Solid, dashed and dotted lines correspond to the decay modes $H^+ \rightarrow W^+ \gamma$, $H^+ \rightarrow W^+ h^0$, $H^+ \rightarrow t\bar{b}$.

$H^+ \rightarrow W^+ \gamma$ branching ratio to a comparatively stable value of 4×10^{-6} . Even for this value, the detectability of point #3 the $H^+ \rightarrow W^+ h^0$ mode is excited, leading to a rapid fall in the $H^+ \rightarrow W^+ \gamma$ branching ratio to about 5×10^{-5} . For even larger values of m_+ the $H^+ \rightarrow t\bar{b}$ mode dominates all others leading to a further fall in the signal is not ruled out, especially at the LHC. For the window $100 \text{ GeV} \leq m_+ \leq m_t + m_b$ one always gets a significant signal of at least a hundred events in a year's run at the SSC and more at the LHC.

Since the dominant contribution to the amplitude is from the diagrams with internal quark lines, QCD corrections could be important. In view of the significant QCD enhancement in the quark loop driven SM process $H \rightarrow gg$, where g is a gluon [13], this point merits further study.

To sum up, we have carefully computed the rare decay mode $H^+ \rightarrow W^+ \gamma$ in the MSSM. This appears to be a useful channel to look for the charged Higgs at the SSC or LHC especially if it is lighter than the top quark. Prospects for seeing this decay if the charged Higgs is heavier than the top quark depend on the other parameters of the model being in the favourable range.

The authors are grateful to G. Bhattacharyya and A. Méndez for discussions. Part of this work was done while A.R. was visiting CERN. He is grateful to the TH Division for its hospitality. S.R. wishes to thank Professor Abdus Salam, the IAEA, UNESCO and the International Centre for Theoretical Physics for hospitality. A.R. would like to acknowledge financial support from the Department of Science and Technology, India and the Department of Atomic Energy, India. The work of S.R. is funded by the University Grants Commission, India.

#3 Radiative corrections to the mass of the H^0 could push up the threshold for the $H^+ \rightarrow W^+ h^0$ mode to $m_+ \geq 170 \text{ GeV}$. At this value, a branching ratio as large as 10^{-3} could be obtained, provided, of course, that the $t\bar{b}$ channel remains kinematically inaccessible.

References

- [1] J.F. Gunion, H.E. Haber, G.L. Kane and S. Dawson, *The Higgs hunter's guide* (Addison-Wesley, Reading, MA, 1990).
- [2] J.F. Gunion, H.E. Haber, F.E. Paige, W.-K. Tung and S.S.D. Willenbrock, *Nucl. Phys. B* 294 (1987) 621; A.C. Bawa, C.S. Kim and A.D. Martin, *Z. Phys. C* 47 (1990) 75.
- [3] G. Jarlskog and D. Rein, eds. *Proc. Large hadron collider Workshop* (Aachen, October, 1990); C.H. Llewellyn Smith, private communication.
- [4] J.F. Gunion, H.E. Haber, S. Komamiya, H. Yamamoto and A. Barbaro-Galtieri, in: *Experiments, detectors and experimental areas for the supercollider*, eds. R. Donaldson and M.G.D. Gilchriese (World Scientific, Singapore, 1988).
- [5] J.F. Gunion, G.L. Kane and J. Wudka, *Nucl. Phys. B* 299 (1988) 231.
- [6] J.A. Grifols and A. Méndez, *Phys. Rev. D* 22 (1980) 1725; A.A. Iogansen, N.G. Uraltsev and V.A. Khoze, *Sov. J. Phys.* 36 (1982) 717; A. Méndez and A. Pomarol, *Nucl. Phys. B* 349 (1991) 369.
- [7] M. Capdequi-Peyranère, H.E. Haber and P. Irulegui, *Phys. Rev. D* 44 (1991) 191.
- [8] G. 't Hooft and M. Veltman, *Nucl. Phys. B* 153 (1979) 365.
- [9] G. Passarino and M. Veltman, *Nucl. Phys. B* 160 (1979) 151.
- [10] J.F. Gunion and H.E. Haber, *Nucl. Phys. B* 278 (1986) 449.
- [11] J. Gasser and H. Leutwyler, *Phys. Rep.* 87 (1987) 77, and references therein.
- [12] S. Raychaudhuri and A. Raychaudhuri, in preparation.
- [13] M. Spira, A. Djouadi and P.M. Zerwas, *Phys. Lett. B* 264 (1991) 440.